Density Functional Study on the Electronic Structure of Trioxorhenium Organyls

Sibylle Köstlmeier, Oliver D. Häberlen, and Notker Rösch*

Lehrstuhl für Theoretische Chemie, Technische Universität München, D-85747 Garching, Germany

Wolfgang A. Herrmann

Anorganisch-chemisches Institut, Technische Universität München, D-85747 Garching, Germany

Bahman Solouki and Hans Bock

Institut für Anorganische Chemie, Universität Frankfurt, D-60439 Frankfurt, Germany

Received August 11, 1995[⊗]

A linear combination of Gaussian-type orbital density functional (LCGTO-DF) investigation of three rhenium−oxo complexes, $RReO_3$ (R = CH_3, η^1-C_6H_5, η^5-C_5H_5), is presented, showing the influence of the three different types of ligand-to-metal bonding σ-alkyl, σ-aryl, and π-aryl, respectively. The calculated ionization potentials of these compounds are compared to their He I photoelectron spectra and found to be in excellent agreement. In particular, the present results for H_3C-ReO_3 are much improved over various other theoretical approaches. Special attention is drawn to the $-ReO_3$ fragment energy levels and to the nonbonding 2p lone pairs on the oxygen atoms; their relative energetic positioning allows conclusions on the charge distribution and thus on the Lewis acidity of the rhenium atom in the active site $-ReO_3$. To assist this interpretation, Mulliken fragment charges and calculated dipole moments are discussed. A recently proposed relationship between the oxygen charge within the $-ReO_3$ fragment and ^{17}O NMR shifts is supported.

1. Introduction

Ligand "tailoring" has long been a major goal in organometallic chemistry. Attempts have been made to quantify both the steric[1−4] and the electronic effects of a ligand on the central metal[5−7] and to obtain correlations with observed chemical and physical properties. In this respect the rhenium−oxo complexes of the type $RReO_3$ represent a model group of compounds, as they exhibit an impressive versatility in their involvement in chemical reactions, depending on the nature of the ligand R. For instance, methyltrioxorhenium, H_3CReO_3, is catalytically highly active in olefin metathesis and epoxidation[8−10] or aldehyde olefination[11] and can be used as a homogeneous or a heterogeneous catalyst. Other $RReO_3$ compounds, however, are stable but catalytically inert, e.g. the cyclopentadienyl complex (η^5-C_5H_5)ReO_3 and its permethylated analogue,[12] or thermally labile or subject to adduct formation with Lewis bases, as is the case for the higher alkyl or phenyl derivatives of the fragment $-ReO_3$.[13]

Theoretical investigations have already been carried out on the electronic structure of some of these compounds.[14−17] Yet, a concise comparison of compounds containing different types of ligands and their influence on the chemical and physical properties, based on results obtained with a selected modern electronic structure method, is still lacking. It should, however, not only be of theoretical interest but may also yield some guidelines for the experimentally working chemist. Here, we will use a recently developed scalar-relativistic variant[18] of the LCGTO-DF method (linear combination of Gaussian-type orbital density functional)[19] method to elucidate the role played by the ligand R on the electronic structure with respect to reactivity and stability. The three compounds chosen for this theoretical investigation differ in both the ligand (alkyl vs aryl) and the bonding type (σ vs π). H_3CReO_3 serves as an

* To whom correspondence should be addressed.
[⊗] Abstract published in *Advance ACS Abstracts,* March 1, 1996.

(1) Tolman, C. A. *Chem. Rev.* **1977**, *77*, 313.
(2) Brown, T. L.; Lee, K. J. *Coord. Chem. Rev.* **1993**, *128*, 89.
(3) Comba, P. *Coord. Chem. Rev.* **1993**, *123*, 1.
(4) Mayer, H. A.; Kaska, W. C. *Chem. Rev.* **1994**, *94*, 1239.
(5) Tolman, C. A. *J. Am. Chem. Soc.* **1970**, *92*, 2953.
(6) Alyea, E. C.; Song, S. *Inorg. Chem.* **1992**, *31*, 4909.
(7) Wilson, M. R.; Liu, H.; Prock, A.; Giering, W. P. *Organometallics* **1993**, *12*, 2044.
(8) Herrmann, W. A.; Wagner, W.; Flessner, U. N.; Volkhardt, U.; Komber, H. *Angew. Chem.* **1991**, *103*, 1704; *Angew. Chem., Int. Ed. Engl.* **1991**, *30*, 1636.
(9) Herrmann, W. A.; Fischer, R. W.; Marz, D. W. *Angew. Chem.* **1991**, *103*, 1706; *Angew. Chem., Int. Ed. Engl.* **1991**, *30*, 1638.
(10) Herrman, W. A.; Fischer, R. W.; Scherer, W.; Rauch, M. U. *Angew. Chem.* **1993**, *105*, 1209; *Angew. Chem., Int. Ed. Engl.* **1993**, *32*, 1157.
(11) Herrmann, W. A.; Wang, M. *Angew. Chem.* **1991**, *103*, 1709; *Angew. Chem., Int. Ed. Engl.* **1991**, *30*, 1641.
(12) Herrmann, W. A.; Ladwig, M.; Kiprof. P.; Riede, J. *J. Organomet. Chem.* **1989**, *371*, C13.
(13) Herrmann, W. A.; Kühn, F. E.; Romão, C. C.; Huy, H. T.; Wang, M.; Fischer, R. W.; Kiprof, P.; Scherer, W. *Chem. Ber.* **1993**, *126*, 45.
(14) Herrmann, W. A.; Kiprof, P.; Rypdal, K.; Tremmel, J.; Blom, R.; Alberto, R.; Behm, J.; Albach, R. W.; Bock, H.; Solouki, B.; Mink, J.; Lichtenberger, D.; Gruhn, N. E. *J. Am. Chem. Soc.* **1991**, *113*, 6527.
(15) Mealli, C.; Lopez, J. A.; Calhorda, M. J.; Romão, C. C.; Herrmann, W. A. *Inorg. Chem.* **1994**, *33*, 1139.
(16) Wiest, R.; Leininger, T.; Jeung, G.; Benard, M. *J. Chem. Phys.* **1992**, *96*, 10800.
(17) Szyperski, T.; Schwerdtfeger, P. *Angew. Chem.* **1989**, *101*, 1271.
(18) Häberlen, O. D.; Rösch, N. *Chem. Phys. Lett.* **1992**, *199*, 491.
(19) Dunlap, B. I.; Rösch, N. *Adv. Quantum Chem.* **1990**, *21*, 317.

0276-7333/96/2315-1872$12.00/0

example for σ-alkyl bonding, the phenyl compound (η^1-H_5C_6)ReO_3 represents σ-aryl bonding, and the cyclopentadienyl complex (η^5-C_5H_5)ReO_3 π-aryl bonding.

2. Computational and Experimental Details

All-electron molecular orbital calculations were carried out using the LCGTO-DF method[19] to solve the effective one-electron equations which result in the Kohn−Sham approach to density functional theory. With the help of the scalar−relativistic variant of the program[18] we were able to self-consistently include relativistic effects (in particular the mass−velocity correction and the Darwin term) in the electronic structure. This method has already been successfully utilized for investigating a variety of compounds containing heavy elements.[20−22] For the exchange-correlation energy functional the local density approximation (LDA) was employed.[23] All valence ionization potentials of H_3CReO_3 and most of the ionization potentials of (η^5-C_5H_5)ReO_3 and (η^1-C_6H_5)ReO_3 were determined from ΔSCF calculations. This approach to the calculation of ionization potentials requires some computational effort and meets with convergence problems in cases of low symmetry and a dense molecular orbital (MO) spectrum, e.g. for the cationic configurations of (η^5-C_5H_5)ReO_3 when the ionization takes place from the MOs 40a′, 39a′, and 36a′ (see below for the MO labeling). Therefore, for these levels of (η^5-C_5H_5)ReO_3 and for the levels 42a′ to 34a′ and 22a″ to 17a″ of the photoemission spectrum of (η^1-C_6H_5)ReO_3 we resorted to Slater's transition state procedure[24] in the approximation that half an electron was removed from the highest lying MO of each symmetry, a′ or a″. For the higher ionization potentials the additional approximation of ionizing only the highest lying MO rests on the assumption of a uniform relaxation of the level manifold. Experience shows that this holds to a good approximation if the spatial characters of the various MOs are similar. The error of this approximation was estimated by checks on various ionization potentials of (η^5-C_5H_5)ReO_3, which resulted in differences in ΔSCF values of typically 0.1 eV for ionization potentials of about 10−13 eV and of up to 0.3 eV for ionization potentials of 14 eV and higher. This somewhat reduced accuracy for higher ionization potentials suffices for an assignment of these parts of the photoelectron spectra. Fragment charges were derived with the help of a Mulliken population analysis.

For Re the construction of the molecular orbital basis set started with a (19/14/10/5) basis,[25] which was augmented by two s exponents (0.01234, 0.19117), three p exponents (0.02335, 0.05838, 0.14595), two d exponents (0.04447, 0.11118), and two f exponents (0.35788, 0.89472). The resulting (21/17/12/7) basis set was contracted to [9/8/5/2]. For C, a (9/5/1) basis set was contracted to [7/4/1]; for H the basis set was (6/1) → [4/1].[26] For oxygen a basis set of type (11/7)[27] was augmented by a d polarization exponent (1.154) and contracted to [6/4/1]. All contractions were of the generalized form based on eigenvectors of the corresponding atomic calculations. The exponents for the polarization functions, d-type for C and O and p-type for H, were taken from ref 28. The fitting basis sets used in the LCGTO-DF method to represent the electron charge density and the exchange-correlation potential have been generated in a standard fashion.[29]

For H_3CReO_3 the Re−C and the Re−O bond distances as well as the umbrella mode of the $-ReO_3$ fragment were optimized in C_{3v} symmetry. They are found to be in very good accordance with experiment (d(Re−O) 1.705 Å calculated, 1.709 Å experimental; d(Re−C), 2.023 Å calculated, 2.060 Å experimental; ∠(O−Re−O) 113.7° calculated, 113° experimental.[14] An optimization of the cyclopentadienyl−Re distance yielded 2.08 Å (experimental 2.06 Å); hence, the experimentally determined geometry[30] is used in the calculations on (η^5-C_5H_5)ReO_3. For the third compound, (η^1-C_6H_5)ReO_3, we chose the experimental structure that can be determined from both the orthorhombic and one of the monoclinic crystal modifications (d(Re−C), 2.01 Å; d(Re−O), 1.71 Å; ∠(O−Re−O), 111°; ∠(C−Re−O), 108°).[31] Experimental values for both the bond lengths and the angles do not vary much in the $RReO_3$ series. Average values for σ-organyl compounds are d(Re−C) 2.04 Å, d(Re−O) 1.69 Å, ∠(C−Re−O) 108° and for π-organyl complexes d(Re−C) 2.07 Å, d(Re−O) 1.71 Å, ∠(centroid−Re−O) 113°).[31]

Helium I photoelectron spectra have been recorded using a high-performance spectrometer (Leybold Heraeus UPG 200). Its resolution, subject to measurement conditions (average intensity usually 1000 cps), is about 20 meV. Spectra calibration is accomplished by adding noble gases (Xe, $^2P_{3/2}$ = 12.13 eV, $^2P_{1/2}$ = 13.43 eV; Ar, $^2P_{3/2}$ = 15.76 eV, $^2P_{1/2}$ = 15.94 eV). The vapor pressure of the compound at the spectrometer inlet amounts to 10^{-2} to 5×10^{-1} mbar and is determined by the temperature of sublimation at the internal spectrometer heating system. After it passes the ionization chamber, the compound is frozen out at a copper metal wall cooled with liquid nitrogen to avoid spectrometer contamination.

All photoelectron spectra have been registered on line using the program package PES, which has been developed by the Frankfurt group and is available on request. It handles well over 50 functions in the recording, manipulation, and compilation of measurement data such as calibration, basis line correction, FFT noise repression, and weighted subtraction from multicomponent spectra.

3. Results and Discussion

Photoelectron spectroscopy is a useful tool to assess the electronic structure of a compound via the sequence of its radical cation states. On the other hand, a variety of computational methods of different levels of sophistication is available to calculate vertical ionization potentials. The interpretation of photoelectron spectra, therefore, is of interest to both experimentalists and theoreticians. Although in special cases complicated by many-electron effects,[32] the assignment of photoelectron spectra within a one-electron approximation, i.e. a molecular orbital framework either by Koopmans' theorem in the Hartree−Fock method or by Slater's transition state concept in the DF approach, is most useful for the experimentally working chemist.

3.1. Methyltrioxorhenium. Before we turn to the assignment of its photoelectron spectrum, a brief description of the ground-state electronic structure of H_3CReO_3 will be given in terms of the Kohn−Sham molecular orbitals as calculated with the LCGTO-DF method. Assuming a pseudo-tetrahedral molecular shape around the rhenium center, we start from the

(20) Rösch, N.; Häberlen, O. D.; Dunlap, B. I. *Angew. Chem.* **1993**, *105*, 78; *Angew. Chem., Int. Ed. Engl.* **1993**, *32*, 108.
(21) Häberlen, O. D.; Schmidbaur, H.; Rösch, N. *J. Am. Chem. Soc.* **1994**, *116*, 8241.
(22) Chung, S.-C.; Krüger, S.; Pacchioni, G.; Rösch, N. *J. Chem. Phys.* **1995**, *102*, 3695.
(23) Vosko, S. H.; Wilk, L.; Nusair, M. *Can. J. Phys.* **1980**, *58*, 1200.
(24) Slater, J. C. *Adv. Quantum Chem.* **1972**, *6*, 1.
(25) Gropen, O. *J. Comput. Chem.* **1987**, *8*, 782.
(26) van Duijeneveldt, F. B. IBM Res. Rep. No. 945, 1971.
(27) Pacchioni, G.; Cogliandro, G.; Bagus, P. S. *Int. J. Quantum Chem.* **1992**, 42, 1115.
(28) Huzinaga, S., Ed. *Gaussian Basis Sets for Molecular Calculations*; Elsevier: New York, 1984.
(29) Jörg, H.; Rösch, N.; Sabin, J. R.; Dunlap, B. I. *Chem. Phys. Lett.* **1985**, *114*, 529.
(30) Kühn, F. E.; Herrmann, W. A.; Hahn, R.; Elison, M.; Blümel, J.; Herdtweck, E. *Organometallics* **1994**, *13*, 1601.
(31) Kühn, F. E. Thesis, Technische Universität München, 1994.
(32) Köppel, H.; Cederbaum, L. S.; Domcke, W.; Shaik, S. S. *Angew. Chem.* **1983**, *95*, 221; *Angew. Chem., Int. Ed. Engl.* **1983**, *22*, 210.

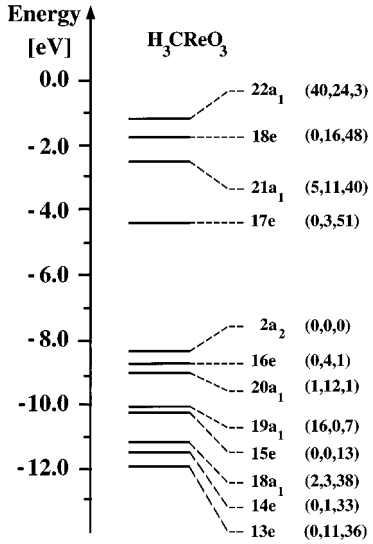

Figure 1. Valence MO energy spectrum of H_3CReO_3 from an LCGTO-DF calculation under C_{3v} symmetry. The levels are filled up to the HOMO $2a_2$. The Re contributions of the levels are indicated in parentheses (s,p,d in percent). Energies are given in eV.

orbital scheme for a tetrahedral molecule and take only the O and C ligand 2p levels into account. In tetrahedral coordination one obtains a set of four orbitals of a_1 and t_2 symmetry for the Re−O and Re−C σ-bonds and another set of eight orbitals for the corresponding π-bonds exhibiting the symmetries e, t_1, and t_2. When the symmetry is reduced to C_{3v}, as is the case in H_3CReO_3, two a_1 orbitals and an e set result for the σ-bonds. The π-bonding orbitals split into a_1, a_2, and three e sets. The energetic ordering of these uppermost eight occupied and the next four unoccupied levels of H_3CReO_3 has been calculated along with the rhenium contributions (s, p, d; see Figure 1) to the corresponding orbital.

The contour plots in the molecular plane H−C−Re−O (Figure 2) depict six of these occupied valence orbitals: the metal−ligand σ-type orbitals 13e, $18a_1$, and $19a_1$ are given on the left-hand side and the π-type orbitals 14e, 15e, and $20a_1$ on the right-hand side (the numbering of the molecular orbitals takes all core levels into account). The σ-bonding MO 13e is mainly centered on the $-ReO_3$ fragment (see Figure 3 for the Mulliken populations, (% R, % Re, % O in parentheses). The next higher MO 14e, in contrast, is π-bonding with respect to all four ligands and delocalized over the whole molecule. The σ-interaction of the $d(z^2)$ orbital on Re both with the oxygen ligands and with the CH_3 moiety is evident in MO $18a_1$. MO 15e is bonding within the CH_3 fragment but π-antibonding with respect to Re−C. A significant metal s contribution of 16% dominates the shape of the σ-bonding $19a_1$ orbital, a consequence of the relativistic contraction of the Re 6s orbital and the concomitant stabilization. Taking into account its Re 6p contribution of 12%, the MO $20a_1$ can be characterized as Re−O π-bonding with some additional stabilization due to overlap with a CH_3 fragment orbital. The two uppermost occupied orbitals, 16e and $2a_2$ (Figure 1), carry oxygen lone pairs.

The large gap of 4.0 eV between occupied and unoccupied levels is typical for a stable closed-shell system. The lowest lying unoccupied MOs 17e, $21a_1$, and 18e

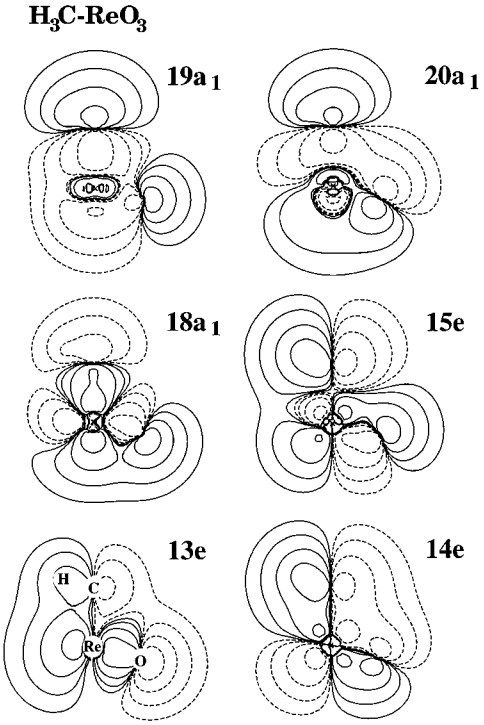

Figure 2. Contour plots for various MOs of H_3CReO_3 in the plane containing the atoms Re and C as well as one H and one O atom: 13e, 14e, $18a_1$, 15e, $19a_1$, and $20a_1$ (see Figure 1). The contour values are 0.0032, 0.0100, 0.0316, and 0.1000 au; solid and dashed lines represent values of opposite sign.

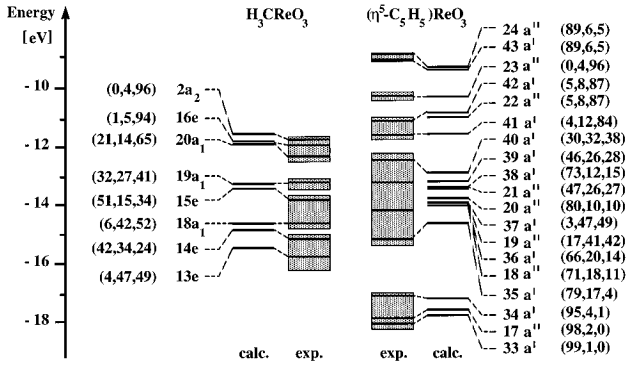

Figure 3. Comparison of the experimental photoelectron spectra of H_3CReO_3 and $(\eta^5$-$C_5H_5)ReO_3$ and the ΔSCF ionization potentials from LCGTO-DF calculations, assuming C_{3v} symmetry for H_3CReO_3 and C_s symmetry for $(\eta^5$-$C_5H_5)ReO_3$. The contributions of the molecular fragments to the calculated levels are indicated in parentheses (R,Re,O in percent). The approximate bandwidths of the He I photoelectron spectra are indicated by shaded areas (see text).

may be formally interpreted as the Re 5d ligand field manifold, whereas MO $22a_1$ may be formally counted as the Re 6s level. All these levels are metal−ligand antibonding. A more detailed inspection of their orbital character reveals that MOs 17e and $21a_1$ are Re−O dominated, whereas MOs 18e and $22a_1$ exhibit a more pronounced CH_3 fragment character. This implies a strong Re−C interaction comprising both σ- and π-type bonding (Figure 2: MOs $18a_1$ and $19a_1$ as well as MOs 13e and 14e).

The photoelectron spectroscopic assignment of H_3CReO_3 has been studied by employing several theoretical approaches of different levels of sophistication.

Table 1. Comparison of the He I Photoelectron Spectrum of H_3CReO_3 and the Calculated Ionization Potentials from Various Theoretical Approaches (Energies in eV)

		LCGTO-		HF-CI[d]			
levels[a]	exptl[b]	DF[c]	FH-Xα[b]	SDCI	ΔSCF	ΔCI	EHT[b]
$2a_2$ ($1a_2$)	11.80	11.62	14.66	11.79	12.36	11.31	14.74
16e (5e)	11.95	11.93	15.70	12.61	13.05	12.04	14.92
$20a_1$ ($5a_1$)	12.35	11.96	15.87	12.60	12.67	12.26	13.94
$19a_1$ ($4a_1$)	13.2	13.28	16.74	13.92			15.11
15e (4e)	13.8	13.36	18.30	14.96			15.22
$18a_1$ ($3a_1$)	14.6	14.66	19.57	16.22			15.42
14e (3e)	15.3	14.95	19.86	16.87			15.67
13e (2e)	(15.8)[e]	15.39	19.86				15.89
Δ_{tot}[f]	3.5	3.3	5.2	5.1			1.7
Δ_{lev}[f]		0.2	4.0	0.9			1.7

[a] The numbering corresponds to the level ordering in all-electron calculations. To facilitate comparison with other calculations, the valence-only numbering is given in parentheses. [b] Reference 14. [c] This work. [d] Reference 16. [e] Shoulder whose maximum cannot be located precisely and was therefore not taken into account in the evaluation of Δ_{tot} and Δ_{lev}. [f] Δ_{tot} is the energy difference between the ionization potentials $2a_2$ and 14e and Δ_{lev} is the average absolute deviation of the calculated ionization potentials $2a_2$ through 14e from the corresponding spectroscopic values.

Table 1 provides a comparison of these previous results with those presented here (Figure 1). Major differences can be observed in two aspects, the total range Δ_{tot} spanned by the valence energy levels under consideration as well as the relative ordering with respect to the symmetry of the corresponding MOs. Several criteria may be applied to assess the overall accuracy of a computational procedure: the energy of the first vertical ionization potential, the average deviation Δ_{lev} between experimental and calculated energy levels, and the energy range Δ_{tot} of the valence ionization potentials under investigation.

In the He I photoelectron spectrum (Figure 4), the first seven peaks span an energy range Δ_{tot} of approximately 3.5 eV between 11.5 and 14.5 eV. This feature is best reproduced by the present scalar-relativistic LCGTO-DF ΔSCF calculations (Δ_{tot} = 3.3 eV), whereas another DF-based method used previously,[14] a Fenske−Hall procedure based on atomic orbitals and energies derived from Xα calculations (FH-Xα), overestimates the splitting by about 1.3 eV. It is difficult to identify possible reasons for this discrepancy between the two DF methods; it may suffice to point out that the present method employs large flexible basis sets in marked contrast to the minimal basis sets used in the FH-Xα approach. In the Hartree−Fock configuration interaction (CI) treatment of H_3CReO_3,[16] ΔSCF and ΔCI calculations have been carried out only for the three lowest lying states of the cationic system, but the SDCI (singles and doubles configuration interaction)-based ionization potentials also exhibit a splitting Δ_{tot} of about 5 eV. On the other hand, with Δ_{tot} = 1.73 eV the extended Hückel scheme clearly underestimates this characteristic feature.[14]

The LCGTO-DF calculation also succeeds if the first vertical ionization potential is taken as a criterion: with a deviation of only 0.18 eV this energy is calculated with very satisfactory accuracy. Only the SDCI and the ΔCI values show comparable or slightly better agreement with experiment, whereas the other methods partially calculate significantly larger values for the first vertical ionization potential.

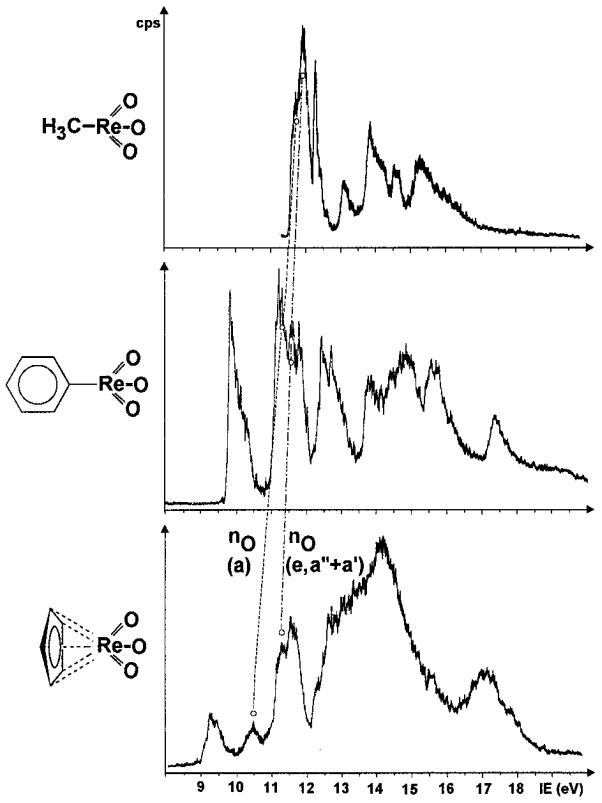

Figure 4. He I photoelectron spectra of methyl-, phenyl-, and (η^5-cyclopentadienyl)trioxorhenium (for calibration and resolution see section 2). The ionizations from the oxygen lone pairs n_O are connected by dashed lines for the a-type combination (C_{3v}, a_2; C_s, a″) and by dot-dashed lines for the degenerate combinations (C_{3v}, e; C_s, a′ + a″).

As far as the assignment of the spectrum is concerned, differences between the various theoretical approaches are encountered for the HOMO and the next two levels (Table 1). The ordering of the remaining four valence levels is found to be $19a_1$ > 15e > $18a_1$ > 14e in all the calculations (i.e. $4a_1$ > 4e > $3a_1$ > 3e, if numbering refers to the valence electron levels only). The two DFT-based methods, LCGTO-DF and FH-Xα, agree on the ordering of the three uppermost occupied orbitals, $2a_2$ > 16e > $20a_1$, with 16e and $20a_1$ being rather close in energy. The HF-ΔCI calculations yield an analogous result, and even in the HF-SDCI scheme, the levels 16e and $20a_1$ (5e, $5a_1$) are essentially degenerate. Deviations are encountered in the HF-ΔSCF calculations proposing the order 16e < $20a_1$. According to the extended Hückel eigenvalues, the $20a_1$ level should be the highest occupied one and a wrong assignment of the ionization sequence results. Moreover, with the average deviation Δ_{lev} per energy level of only 0.22 eV between the calculated and the measured ionization potentials for the observed seven peaks, the LCGTO-DF description of the H_3CReO_3 spectrum is in very satisfactory agreement with experiment, much improved over all previous computational treatments (Table 1). In conclusion, it is clear how well the LCGTO-DF calculations reproduce the intensity pattern of the He I photoelectron spectrum, including the two major groups of peaks (see Figures 3 and 4).

3.2. (η^5-Cyclopentadienyl)trioxorhenium. The recently recorded photoelectron spectrum of (η^5-C_5H_5)-ReO_3, in contrast to that of H_3CReO_3, exhibits five groups of partially overlapping bands. The less pro-

nounced peak resolution is due to the higher level density of the organic ligand $C_5H_5^-$. The He I valence ionization energies span a range of about 9 eV, starting at 9 eV.

The nonbonding oxygen lone pairs (MOs 23a″, 42a′, 24a″) of the π-compound (η^5-C_5H_5)ReO_3 account for the second and third peaks at 10.5 and 11.4 eV. The character of the level 23a″ is in exact correspondence with that of the $2a_2$ HOMO of H_3CReO_3, except it is shifted upward in energy by about 1.3 eV, which matches the experiment quite closely. In accordance with H_3CReO_3, some orbitals (40a′, 39a′, and 21a″) delocalized over the whole molecule are predicted to follow at about 13.0 eV. Yet, in the cyclopentadienyl derivative they are already preceded by one of the $-ReO_3$ fragment orbitals (Figure 3: MO 41a′). As for two other distinct ReO_3 orbitals (Figure 3: 37a′ and 19a″), this MO is upward-shifted in energy even more than the oxygen lone pairs with respect to their H_3CReO_3 analogs (by 2.5 eV on the average). This indicates that the $-ReO_3$ fragment as a whole is more negatively charged in the π-cyclopentadienyl derivative than in the methyl derivative and that this additional electronic charge is likely to be localized more on the rhenium center, because the oxygen lone pair levels remain almost constant (Figure 4; dotted lines). As a consequence, reactions depending on a Lewis acidic Re center should be either inhibited or at least severely hindered. Some π-type levels of the cyclopentadienyl ligand contribute to the rather broad fourth peak, as well (Figure 3; MOs 38a′, 36a′, 35a′, 20a″, 19a″, and 18a″). The total energetic splitting of approximately 3.5 eV can be compared to that for H_3CReO_3, although an average upward shifting by 1.4 eV is observed.

These three bands in the middle part of the spectrum are similar to those of H_3CReO_3 and are flanked by two further peaks, one at higher and one at lower energy (see Figure 4, bottom), which represent almost pure cyclopentadienyl levels. The HOMO group, MOs 24a″ and 43a′ (Figure 3), is energetically nearly degenerate and of ligand π-type, and the fifth band at 17−18 eV belongs to σ-type orbitals within the C_5H_5 skeleton. With Δ_{tot} = 8.6 eV the present DF calculations slightly underestimate the experimentally observed level splitting of about 9 eV; nevertheless, considerably better agreement is achieved than with the orbital eigenvalue spectrum derived in a HF pseudopotential calculation, Δ_{tot} = 7.5 eV.[17]

3.3. (η^1-Phenyl)trioxorhenium. In the He I photoelectron spectrum of (η^1-C_6H_5)ReO_3 five major band regions are observed (see Figure 4): around 10 eV, from 11.0 to 12.0 eV, from 12.2 to 13.2 eV, from 13.5 to 16.3 eV, and around 17.2 eV. The calculated ionization pattern (Figure 5) is less well structured because energy levels of the phenyl ligand are assigned throughout the whole spectral range, but the above-mentioned five bands may be discriminated as well. The mixing of the ligand levels with the $-ReO_3$ fragment is more pronounced than in H_3CReO_3 and in (η^5-C_5H_5)ReO_3. As an example, one may consider the highest occupied level 45a′ which is basically of ligand π-character but has a ReO_3 admixture of 10%. The next lower level 25a″ is of pure ligand π-type. In comparison to (η^5-C_5H_5)ReO_3, the lowest ligand based ionization potential is found at a higher energy, 10.0 eV (Figure 4: (η^5-C_5H_5)ReO_3 9.4 eV).

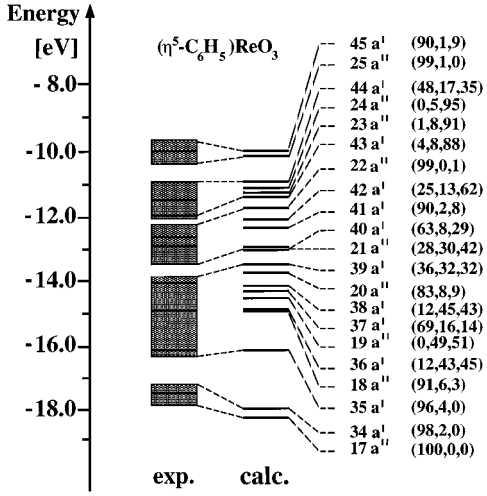

Figure 5. Comparison of the He I photoelectron spectrum of phenylrhenium trioxide and the corresponding LCGTO-DF ionization potentials (in eV) obtained from ΔSCF and transition state calculations assuming C_s symmetry (see section 2). The dominant radical cation state contribution to the calculated orbitals is indicated in parentheses (R,Re,O in percent).

This band group of lowest ionization potentials is energetically separated from the nonbonding oxygen 2p levels 24a″, 23a″, and 43a′ by about 1 eV. The calculated ionization potentials corresponding to the latter levels are comparable to those obtained for H_3CReO_3 (11.2, 11.4, and 11.5 eV vs 11.6 and 11.9 eV in H_3CReO_3) with a trend to higher values. With MO 44a′ even one of the rather delocalized orbitals of π-type bonding between Re and O is found within this second group of ionization potentials, which spreads from 11.0 to 11.6 eV, in quite good agreement with the experimental values.

In the calculations the third and the fourth band groups follow with almost no energetic spacings and extend from 11.8 to 13.2 eV and from 13.6 to 16.3 eV. With the MOs 42a′, 21a″, and 39a′ three orbitals found in this region are delocalized over the whole molecule. Four orbitals of almost pure ligand π-type are encountered here with 22a″, 20a″, 18a″, and 41a′, whereas the ligand-dominated orbitals 40a′ and 37a′ contain a higher ReO_3 admixture.

Probably the most interesting features in this energy region, however, are again the π-bonding ReO_3-based levels 21a″ and 39a′ around 13.4 eV, obviously mixing with 44a′ at 11.0 eV, and the σ-bonding ReO levels 38a′, 19a″, and 36a′ corresponding to ionization potentials around 14.5 eV. From 15 eV on and at about 18.2 eV the present calculations yield two further ionization potentials from pure ligand levels, 34a′ and 17a″, that are of C−H bonding character.

Altogether the correlation of experimental and calculated ionization energies for (η^1-C_6H_5)ReO_3 is rather satisfactory and the ΔSCF deviations are acceptably small (Figure 5).

For the analysis of the interaction between phenyl and $-ReO_3$ it is instructive to shift the point of view, considering the $-ReO_3$ fragment as a substituent of the organic moiety. Such a substituent group at the phenyl ring can be characterized with respect to its donor or acceptor properties by π perturbation of the phenyl

Table 2. Calculated Ionization Potentials (IEs) of Characteristic Orbitals of the Compounds H_3CReO_3, (η^1-C_6H_5)ReO_3, and (η^5-C_5H_5)ReO_3 (in eV)

	MTO		$PhReO_3$		$CpReO_3$	
	orbital	IE	orbital	IE	orbital	IE
O p	$2a_2$	11.6	24a″	11.2	23a″	10.2
	16e	11.9	23a″	11.4	42a′	10.8
			43a′	11.5	22a″	11.0
Re−O σ	$18a_1$	14.7	38a′	14.1	41a′	11.7
	13e	15.4	19a″	14.6	19a″	13.8
			36a′	15.0	37a′	14.1
Re−O π	$20a_1$	12.0	44a′	11.0	40a′	13.1
	15e	13.4	21a″	13.2	39a′	13.2
			39a′	13.6	21a″	13.2

radical cation states[33] or, in the context of a density functional method, of the Kohn−Sham molecular orbitals in combination with Slater's transition state concept.[24] An estimate may be based on the photoelectron spectrum of trioxo(η^1-mesityl)rhenium(VII):[14] the two lowest vertical ionizations are measured or identified by band analysis at 9.0 and ∼9.3 eV; i.e. they are shifted by about 0.5 and ∼0.8 eV relative to the degenerate ones of the hydrocarbon mesitylene (D_{3h}), $IE_{1,2}(e) = 8.47$ eV.[34] This rather strong acceptor property of a $-ReO_3$ group is further substantiated by the photoelectron spectrum of the phenyl derivative presented here (Figures 4 and 5), which allows us to read off $IE_1^v = 9.84$ eV and $IE_2^v \sim 10.1$ eV, values increased relative to those of benzene (D_{6h}) at $IE_{1,2}(e_{2g}) = 9.24$ eV,[34] by 0.6 and ∼0.9 eV. The practically identical shifts prove experimental reliability and, above all, that the group $-ReO_3$ is a rather strong ($\pi + \sigma$) acceptor at appropriate positions of a π-hydrocarbon. In addition, as is demonstrated by the n_O lone pair ionizations (Figure 4: dashed and dot-dashed lines), which are lowered in energy, the σ-electron density withdrawal exceeds the π-back-donation within a first- and second-order perturbation model.[33]

3.4. Charge Distribution in Trioxorhenium Organyls. A comparison of the ionization potentials from some characteristic orbitals of the three compounds under investigation (Table 2) provides interesting insight. We chose the oxygen lone pairs and both the π and the σ bonds between rhenium and oxygen, which show comparable ligand to ReO_3 ratios in all three molecules. For the pure ligand orbitals, a direct comparison of the ionization potentials is hampered by the ligand topologies being too different. As a general feature, however, π-type orbitals yield ionization potentials between 9 and 10 eV, whereas σ-type orbital ionizations exceed 13 eV.

For all the orbitals considered (Table 2) a uniform trend toward lower ionization energies is calculated in the series H_3CReO_3 > (η^1-C_6H_5)ReO_3 > (η^5-C_5H_5)ReO_3 that indicates the increasing amount of electron charge transfer to the $-ReO_3$ fragment concomitant with the higher electron-donating character of the ligand in the ordering $CH_3 < C_6H_5 \ll C_5H_5$. Yet, some differences in the electron-donating properties can be discriminated: In (η^5-C_5H_5)ReO_3, the ionization potential 41a′, which is most strongly lowered relative to the corresponding ionization potential of H_3CReO_3, exhibits Re−O σ bonding character. In (η^1-C_6H_5)ReO_3, on the other hand, charge donation occurs via the π-channel, because of the favorable overlap of a ring carbon π-orbital with the corresponding rhenium d(π) orbital, 44a′, which exhibits additional π-type interactions with oxygen p orbitals. This underlines a qualitative similarity between the σ-aryl-bonding phenyl ligand and the σ-alkyl-type methyl ligand in H_3CReO_3, for which the calculation yielded some π-interaction between a carbon p orbital and the corresponding metal d orbital (see section 3.1). Finally, it is worth noting that for (pseudo) tetrahedral symmetry a labeling of orbitals as σ or π faces the problem that both interaction channels contribute to the same irreducible representation, e.

Table 3. Correlation between Mulliken Charges on the $-ReO_3$ Fragment and ^{17}O NMR Shifts (Charges in au and Shifts in ppm)

	$MeReO_3$	$PhReO_3$	$CpReO_3$	ReO_4^-
q(R)[a]	0.01	0.09	0.17	
q(Re)[a]	0.37	0.27	0.28	0.00
q(O)[a]	−0.12	−0.12	−0.15	−0.25
^{17}O NMR[b]	829	856	691	562

[a] This work. [b] Reference 30.

To assist this interpretation of the electronic structure, molecular dipole moments μ and Mulliken charges have also been calculated (Table 3). For H_3CReO_3, the present calculation yields a somewhat higher value, 3.10 D, than for experiment, 2.6 D.[14] In contrast, for (η^5-C_5H_5)ReO_3 the agreement is quite satisfactory, 5.58 D (calculated) vs 5.8 D (experiment).[31] For (η^1-C_6H_5)ReO_3 a dipole moment of 4.45 D is predicted, but no experimental value is available. On the basis of the experimental result, that the main geometrical features of the three compounds do not vary much, the value of the dipole moment can be interpreted to reflect the amount of electron donation from the ligand to the $-ReO_3$ fragment. The ordering $\mu(H_3CReO_3) < \mu$((η^1-C_6H_5)ReO_3) < μ((η^5-C_5H_5)ReO_3) confirms the trend deduced from the lone pair ionization potentials. Additionally, the dipole moment for the $-ReO_3$ fragment was calculated to be 1.98 D, which corroborates the dipole moment increment, 2.2 D, derived from the comparison of several rhenium compounds.[35]

The Mulliken analysis of the calculated charge density for various compounds further supports these conclusions (Table 3). The positive charge of the ligand groups increases in the order $H_3C < \eta^1$-$C_6H_5 < \eta^5$-C_5H_5. The rhenium center bears the highest positive charge in H_3CReO_3 with +0.37 au, whereas in (η^1-C_6H_5)ReO_3 and in (η^5-C_5H_5)ReO_3 its positive charge is reduced by about 0.1 au. Although Mulliken charges have to be viewed with due caution, these findings clearly indicate that, due to electron "donation" from the organic and the oxygen ligands, the charge on the metal atom is far below the value corresponding to the formal oxidation state of +VII. Additionally, the larger upward shift of the nonbonding oxygen 2p levels in (η^5-C_5H_5)ReO_3, which is expected to correlate with a higher amount of charge density located on oxygen, reflects the corresponding Mulliken charges on oxygen rather well.

Experimentally, the oxygen charge can be indirectly monitored by NMR measurements. As the rhenium nucleus does not allow for NMR investigations, ^{17}O NMR spectra of various complexes $RReO_3$ have been

(33) Bock, H. *Angew. Chem.* **1989**, *101*, 1659; *Angew. Chem., Int. Ed. Engl.* **1989**, *28*, 1627.
(34) Bock, H.; Kaim, W. *Chem. Ber.* **1978**, *111*, 3552.
(35) Fischer, E. O.; Schreiner, S. *Chem. Ber.* **1959**, *92*, 938.

studied in detail.[30,36] Both H_3CReO and $(\eta^1\text{-}C_6H_5)ReO_3$ yield peaks at a low field of $\delta(^{17}O)$ 829 ppm and $\delta(^{17}O)$ 856 ppm, respectively, whereas the $(\eta^5\text{-}C_5H_5)ReO_3$ signal is found at $\delta(^{17}O)$ 691 ppm, and for the anion ReO_4^- a value of $\delta(^{17}O)$ 562 ppm is obtained (Table 3). Frequently, low-field shifts are interpreted to be connected to a deshielding of the NMR nucleus of an electron-deficient center and, vice versa, a shift to higher field to an increase in electronic charge on the center under concomitant with an enlarged shielding. This qualitative picture is supported by the present calculations. The two compounds with signals at low field, H_3CReO_3 and $(\eta^1\text{-}C_6H_5)ReO_3$, exhibit the smallest negative charge on the oxygen centers (−0.12 au), which in $(\eta^5\text{-}C_5H_5)ReO_3$ are already somewhat more negative, and for the perrhenate anion both the highest amount of negative charge (−0.26 au) is computed and the smallest low-field shift is observed.

4. Conclusions

The present density functional results for the ionization potentials of H_3CReO_3 compare favorably with the results of various other theoretical investigations. Only minor deviations from the absolute values of the experimental He I ionization potentials of H_3CReO_3 are encountered both for the total splitting of the levels and for their relative energetic positioning. Satisfactory agreement with the experimental spectra is also obtained for $(\eta^5\text{-}C_5H_5)ReO_3$ and $(\eta^1\text{-}C_6H_5)ReO_3$. From the relative positioning of the orbitals located on the ReO_3 moiety it is concluded that the electron charge density on the $-ReO_3$ fragment increases in the order CH_3ReO_3 < $(\eta^1\text{-}C_6H_5)ReO_3$ < $(\eta^5\text{-}C_5H_5)ReO_3$. This holds in particular for the valence electron density on the rhenium center but, to a lesser degree, also for the oxygen centers. These deductions are further supported by the calculated dipole moments, which exhibit a consistent change in size. An examination of the Mulliken charges on the rhenium and the oxygen centers corroborates this rationalization as well as a recently proposed relationship between the negative charge on the oxygen ligands and the chemical shift observed in ^{17}O NMR investigations: the smaller the charge on oxygen, the lower the field at which the NMR signals occur.

From the electronic structure point of view, the reactivity of the H_3CReO_3 molecule is correlated with the higher Lewis acidity of the rhenium center compared to the other model compounds. In $(\eta^5\text{-}C_5H_5)ReO_3$ the reactivity is blocked by the larger amount of charge donated from the cyclopentadienyl ring to the $-ReO_3$ fragment. This is probably due to the higher hapticity η^5-bound complexes, which helps to distribute a positive charge over the whole ligand and increases electron donation. For the effect of methylation on benzene, one can easily deduce that the permethylated compound $(\eta^5\text{-}C_5(CH_3)_5ReO_3$ should be even more stable, in agreement with experiment.[30] Not unexpectedly, the σ-aryl compound $(\eta^1\text{-}C_6H_5)ReO_3$ resembles more strongly the σ-alkyl H_3CReO_3 than the π-aryl derivative $(\eta^5\text{-}C_5H_5)ReO_3$. Nevertheless, $(\eta^1\text{-}C_6H_5)ReO_3$ is known to form stable adducts with Lewis bases.[37] A bulkier σ-aryl ligand, mesityl for instance, suppresses the base adduct formation but also deactivates the rhenium center by its enhanced donor strength. These aspects clearly call for additional investigations directly targeting steric effects.

In summary, the present study elucidates the electronic structure of molecules $RReO_3$, which comprise an important class of organometallic compounds. Combining photoelectron spectroscopy and density functional calculations, a coherent rationalization for the interaction of the $-ReO_3$ moiety with σ-alkyl, σ-aryl, and π-aryl ligands is achieved.

Acknowledgment. This work has been supported by the Deutsche Forschungsgemeinschaft, by the Bayerische Forschungsverbund Katalyse, and by the Fonds der Chemischen Industrie.

OM9506375

(36) Herrmann, W. A.; Kühn, F. E.; Roesky, P. W. *J. Organomet. Chem.*, in press.

(37) de Méric de Bellefon, C.; Herrmann, W. A.; Kiprof, P.; Whitaker, C. R. *Organometallics* **1992**, *11*, 1072.